中國機械工程學刊第四十三卷第五期第 431~440 頁(民國一百一十一年)
Journal of the Chinese Society of Mechanical Engineers, Vol.43, No.5, pp.431~440 (2022)

A Study on Hot Stamping of Tailor Welded Blanks

Chien-Hsing Lee*, Ching-Hua Hung**, Ping-Kun Lee ***, Cheng-Kai ChiuHuang *** and Fuh-Kuo Chen****

Keywords: hot stamping, tailor welded blank, U- hat-shaped specimen, three-point bending test, half-section B-pillar, energy absorption.

ABSTRACT

The automotive industry is constantly seeking to reduce the weight of vehicles without compromising safety. Effectively resisting side crashes requires that the B-pillars in automobiles possess high energy absorption capacity in their base area while retaining the martensitic structure to prevent deformation in the upper area. This has led to the development of tailor welded blanks (TWBs), in which a single automobile structural panel possesses a variety of mechanical properties. This study involved a series of experiments on the hot stamping of tailor welded blanks, including U-hat-shaped specimens and half-section B-pillars. In experiments, three-point bending tests revealed that the energy absorption capacity of the TWB test pieces was directly proportional to the strength of the constituent materials. It was also determined that it is possible to fabricate low-weight TWBs comprising high-strength and low-strength materials to guide structural parts' resistance and deformation behavior to achieve the characteristics required for crashworthiness.

INTRODUCTION

Advanced high-strength steel is increasingly being used in the fabrication of lightweight body components to enhance vehicle performance and energy efficiency; however, stamp forming at room temperature can lead to spring back (Xing et al., 2009), distortion, and other adverse effects.

Hot stamping was first developed in the early 1970s. Essentially, manganese–boron steel is heated to 930 °C and held at that temperature for 3–5 minutes to convert the metallographic structure from ferrite into austenite. The blank is then deformed in a die and quenched to below 200 °C before the die is opened. When the average cooling rate exceeds the critical quenching rate of 27°C/s, the austenitic microstructure in the stamped portion is converted into a martensitic microstructure with a tensile strength exceeding 1500 MPa (Karbasian et al., 2010). Bariani et al. (2008) studied the formability of hot-stamped high-strength steel blanks.

Hot stamping of high-strength steel is one approach to reducing vehicle weight (Eller et al., 2014). However, with limited ductility of typically 6%~8% elongation, the resulting high-strength regions lack the ductility and energy absorption required to protect occupants from vehicular impacts (Li et al., 2014; Taylor et al., 2018). The complete martensitic parts are characteristic of high strength and poor ductility generally. Therefore, generally high strength steel hot stamped parts are not suitable for the energy-absorbing parts of automobiles (Wang et al., 2014). This has led to the development of tailor welded blanks (TWBs) specifically for safety-related automotive parts; wherein a single blank possesses high strength to resist deformation and low strength to absorb impact energy. TWB combines different sheet thicknesses and steel grades in the same blank. This solution has the advantage of locally adjusting the material thickness, strength, and elongation to control the deformation modes in crash situations (Hein et al., 2008). Tailored components having a total elongation of about 30% in the high ductility zone were hot-stamped from TWB composed of 22MnB5 and 270 MPa sheets (Mori et al., 2020). Taylor et al. (2018) suggested that a partially martensitic microstructure steel possessing a yield stress of about 350 MPa, an ultimate tensile stress of about 500 MPa, and a total elongation of about 25% is suitable for the soft zone material, such as the MBW500 introduced by ThyssenKrupp Steel AG.

Paper Received April, 2022. Revised May, 2022. Accepted July, 2022. Author for Correspondence: Fuh-Kuo Chen

** Ph.D. Student, Department of Mechanical Engineering, National Yang-Ming Chiao Tung University, Address: Hsinchu, 30010, Taiwan, ROC.*

***Professor, Department of Mechanical Engineering, National Yang-Ming Chiao Tung University, Address: Hsinchu, 30010, Taiwan, ROC.*

**** Product Application Research Section, Iron & Steel Research & Development Department, China Steel Corporation, Address: No. 1, Chung Kang Rd., Kaohsiung 81233, Taiwan, ROC.*

***** Professor, Department of Mechanical Engineering, National Taiwan University, Address: No. 1, Sec. 4, Roosevelt Rd., Taipei 10617, Taiwan, ROC. (corresponding author)*

They further indicated that MBW500 has a chemical composition comparable to high-strength low-alloy (HSLA) steel HC340LA.

Merklein et al. (2014) designated four types of tailored hot-stamped blanks. Karbasian et al. (2010) designated five tailored hot stamping methods, including tailor-welding and tailor-rolling patchwork fabrication, tailored heating, tailored quenching, and tempering using partitioning. After hot stamping tailor welded blanks, Tang et al. (2013) determined that boron steel can be welded to high-strength low-alloy steel (HSLA) to create complex components with high local deformability (Bok et al., 2015). Most previous research on the welding of boron steels has focused on HSLA steel (Merklein et al., 2014), Ductibor® 500P (Múnera et al., 2009), or 340Y (Choi et al., 2012). Kolleck et al. (2015) examined the weld properties of components fabricated via hot stamping from tailor welded blanks. Choi et al. (2016) reported the formation of a heat-affected zone near the weld bead of laser-welded 22MnB5 steel sheets. They also determined that hot stamping can profoundly affect high-hardness martensite in these areas. Peister et al. (2017) reported that in TWB Usibor1500-AS / Ductibor500-AS components fabricated in a U-hat-shaped hot stamping die, the width of the transition zone between the hard and soft zones was less than 2 mm.

Hot stamping has been widely adopted to fabricate tailor welded B-pillars in automobiles, wherein the hard area prevents invasion during the collision while the soft area absorbs kinetic energy (Song et al., 2015). This approach also reduces the complexity of fabrication (George et al., 2012). For example, in the rear rail and B-pillar of the Audi A4/A5 (SOP 2007), 22MnB5 is welded to HSLA. Note that an optimal B-pillar design can also reduce the vehicle's weight by up to 12.1% (Li et al., 2014).

Three-point bending tests can be performed using simulations (Pack et al., 2016) or experiments. Peister et al. (2018) reported no weld failures in Usibor1500-AS/Ductibor500-AS TWBs. A ductile sheet (i.e., backing blank) is generally spot welded to the bottom of a U-shaped blank in assembly-line production. The method has proven effective in ensuring joint strength (Pack et al., 2016; Tang et al., 2020). Merklein et al. (2016) discussed the process of manufacturing tailored B-pillars using laser-welded blanks fabricated with strict control over the die quenching rate. Li et al. (2014) investigated the mechanical properties and energy absorption performance of hot-stamping door impact beams. The finite element analysis is a reliable approach to deriving punch load-displacement curves from the results of three-point-bending tests. Researchers have also determined that TWBs do not have a deleterious effect on the dimensional accuracy of components (ChiuHuang et al., 2020). Note, however, that the effect of TWBs on the energy absorption capacity of hot-stamped parts has rarely been discussed.

In this study, a series of TWB hot stamping experiments were first conducted for forming U-hat-shaped specimens, followed by three-point bending tests. The experimental results obtained from three-point bending tests were then used to compare the energy absorption performance of various TWBs versus conventional U-hat-shaped hot stamped parts. This study also examined the material characteristics of a half-section B-pillar produced by hot stamping a TWB. The research results provide a valuable reference for the design of the hot stamping of TWBs.

EXPERIMENTS

Material properties

Arcelor Mittal produces a TWB hot stamping B-pillar combining a hard zone material of Usibor 1500P and a soft zone material of Ductibor 500P. The strength of the hard zone material can reach 1400 MPa, and the strength of the soft zone material is roughly 460~700 MPa (Arcelor Mittal, 2016).

This study focused on CSC-15B22 (15B22, China Steel Co., Taiwan) in manufacturing tailor welded blanks. The surface-coated manganese-boron steel 15B22 was used as the hard zone material. The material properties of 15B22 are very similar to those of 22MnB5, and the alloy compositions of both materials are listed in Table 1 (Chen et al., 2018; Mu et al., 2018).

Table 1. Alloy compositions of coated 15B22 and 22MnB5 (wt%)

Steel	C	Si	Mn	P	S	B
coated 15B22	0.19-0.25	0.15-0.25	1.05-1.35	<0.02	<0.01	<0.003
coated 22MnB5	0.23	0.25	1.35	0.006	0.005	0.003

The main requirements of tailor welded blanks in the soft zone are good ductility and resistance to morphological changes during the hot stamping process. This prompts the selection of 340LA and 440W as soft zone materials, the strength and elongation of which are expected to fall within the scope of application requirements after hot stamping, as suggested by Taylor et al. (2018). A higher strength steel 590Y with a low elongation after hot stamping was also selected as soft zone material for the energy absorption comparison purpose. The hard and soft materials were then employed in a series of experiments involving the hot stamping of tailor welded blanks. The material properties of hard and soft materials before and after hot stamping are shown in Table 2. It is observed that the strength and elongation of both 340LA and 440W do not exhibit notable changes before and after hot stamping, remaining high elongations of 27.3% and 24.6%, respectively. In contrast, both 15B22 and 590Y display a relatively low elongation of 7.8% after hot stamping.

Table 2. Material properties of hard and soft materials before and after hot stamping

Material properties		YS (MPa)	TS (MPa)	EL (%)
before hot stamping	340LA	340	410	21
	440W	265	440	27
	590Y	260	590	18
after hot stamping	15B22	1095	1555	7.8
	340LA	378	529	27.3
	440W	339	482	24.6
	590Y	798	1035	7.8

Experimental equipment

An 800-ton hot-stamping press (LD-800, Metal Industries Research & Development Centre, MIRDC, Taiwan), as shown in Fig. 1, is employed to stamp all the test specimens and a half-section B-pillar with TWB. A heating furnace supplied by MIRDC is also adopted to heat the TWB. After the test specimens are stamped, a three-point bending test equipment (MTS-370, MTS Systems, USA), as shown in Fig. 2, is used to assess the structural strength.

Fig. 1. 800-ton hot-stamping press

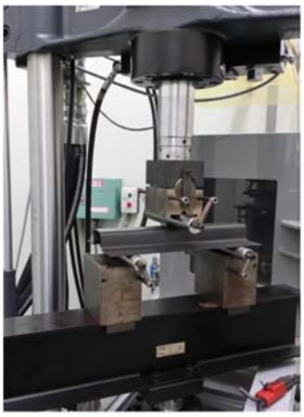

Fig. 2. The three-point bending test experiment

Experiment processes and data measurement in strength tests

As shown in Fig. 3, specimens were prepared using steel with a uniform structure (single property) or tailor-welded structure (multiple properties). The blanks measured 320 mm × 200 mm × 1.4 mm. The uniform specimens included 15B22, 340LA, 440W, and 590Y. The materials used for the hard and soft zones of the tailor-welded blanks were as follows: 15B22+340LA, 15B22+440W, and 15B22+590Y, as shown in Fig. 4. The tailor-welded specimens were fabricated via laser welding parallel to the narrow side (transverse weld) or parallel to the longer side (longitudinal weld) to investigate the effects of weld location on bending strength. The hot stamping process was performed first for all the prepared specimens according to the production forming conditions, including heating, transfer, stamping, and die quenching.

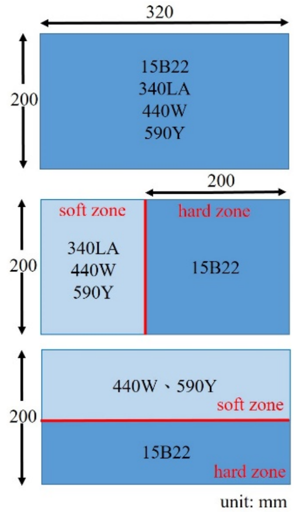

Fig. 3. Dimensions of a single property blank and TWB specimens

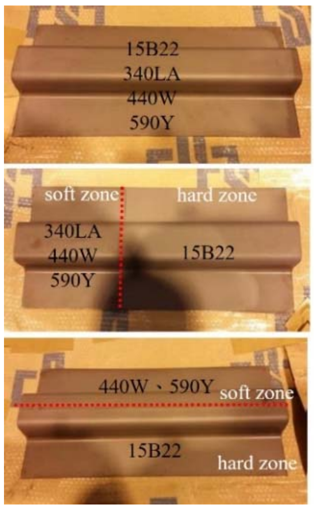

Fig. 4. TWB panels with transverse and longitudinal welds

The three-point bending tests were then conducted. In the three-point bending test, a U-hat-shaped specimen is placed on two supporting rollers, and a roller punch moves down transversely with a 50 mm/min speed to bend the specimen, as shown in Fig. 2. The supporting rollers with a diameter of 30.8 mm are located 220 mm apart, and the centerline of the punch was located in the hard area, at a distance of 40 mm from a welding line. The punch pressure and displacement were recorded throughout the experiment.

Most side impacts involve a strike in the lower half of the B-pillar (Wang et al., 2015; Shi et al., 2022); therefore, transverse welding is commonly offset from the center of the component by 40mm. The hard zone is thus designed to be 200mm, and the soft zone is designed to be 120mm. In this study, the finite element software PAM-STAMP was used to simulate the three-point bending tests. The simulation models for the bending tests are shown in Fig. 5, in which the three rollers are set to be rigid bodies with the supporting rollers fixed and the punch moving transversely down at a velocity of 50 mm/min as the boundary conditions. The true stress-strain curves of the four materials used in the simulations are displayed in Fig. 6, and the process parameters are shown in Table 3.

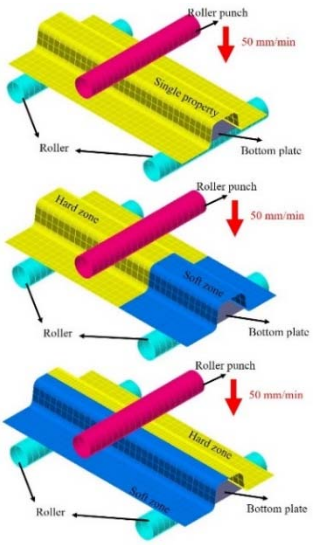

Fig. 5. FEM models of three-point bending test

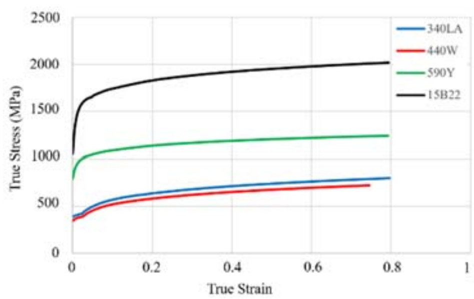

Fig. 6. True stress-strain curves of hard and soft materials

Table 3. Process parameters used in FEM simulation of three-point bending test

Specimen thickness (mm)	1.4
Specimen length (mm)	320
Bottom plate material	980Y
Bottom plate thickness (mm)	1.2
Roller punch speed (mm/min)	50
Roller punch diameter (mm)	30.8
Distance between two roller support points (mm)	220

The maximum bending loads and energy absorptions of the test specimens obtained in the three-point bending tests were compared. Figure 7 shows deformed U-hat-shaped specimens after testing. To prevent the opening of the sidewall during punch loading, a 980Y/1.2t steel plate was spot welded on the bottom side of some of the specimens. Specimens with the plate were designated closed groove specimens, whereas those without the plate were designated open groove specimens.

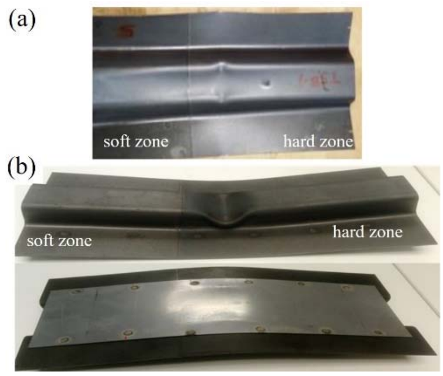

Fig. 7. U-hat-shaped specimen after three-point bending test, (a) opening groove specimen, (b) closed groove specimen

A half-section B-pillar was used to investigate the mechanical properties of hot-stamped TWBs using 340LA, 440W, or 590Y as the soft zone material (thickness of 1.4 mm). Figure 8 presents a cross-section diagram showing the shape and size of the B-pillar. After hot stamping, the test pieces were cut in multiple positions to assess the mechanical properties.

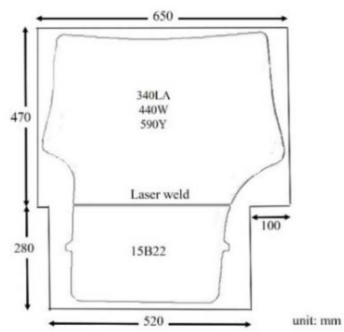

Fig. 8. Dimensions of a half-section TWB B-pillar

EXPERIMENT RESULTS AND DISCUSSIONS

Three-point bending test: Uniform blank

Figure 9 presents uniform blanks after the three-point bending test. The hardest material was 15B22, as indicated by a nearly complete lack of bending deformation. The next harder material was 590Y, followed by 340LA and 440W, as noted in the extent of deformation.

Figure 10 presents TWB 15B22+340LA, 15B22+440W, and 15B22+590Y samples with transverse and longitudinal welds after the bending test. The soft zones appeared flattened, while the hard zone retained the shape of the open groove, thereby fulfilling the functional requirement of TWB B-pillars. The deformation of the soft zone in transverse welded 15B22+590Y was hindered by the mechanical strength of the material. The groove of the longitudinally welded specimens opened up under compressive load, resulting in fracturing along the weld line. Clearly, the strength of 590Y was too high for this test; however, the selection of soft and hard materials depends on the practical strength requirements of the component.

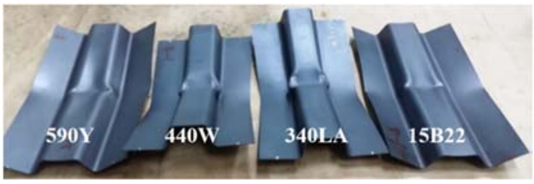

Fig. 9. Experimental results for the single property blank with opening groove

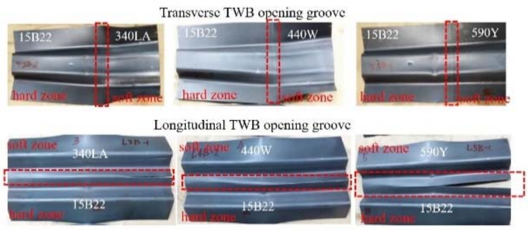

Fig. 10. Experiment results of transverse and longitudinal welded TWBs with an open groove. The area between the red-dashed lines indicates the weld zone

Figure 11 presents the results of the three-point bending test on closed groove blanks with a steel plate welded on the bottom side of the specimen. The area under the punch displacement curve represents the energy absorption capacity. Figure 11(a) illustrates the three-point bending results of a uniform blank, indicating that the reaction force of the punch increased proportionally with the strength of the material. The samples were ranked in punch force from high to low: 15B22, 590Y, 340LA, and 440W. Figure 11(b) presents experiment results of TWBs with a transverse weld line. It was observed that the curve of TWB 15B22+590Y was similar to that of uniform 15B22 due to the fact that the punch was in contact with the hard 15B22 material during three-point bending. Clearly, the grade of the hard zone material determined the performance of the specimen in the three-point bending test. After punch displacement of 30 mm, the punch force of the TWB 15B22+440W sample began to decrease, indicating that the soft zone material affected the energy absorption characteristics.

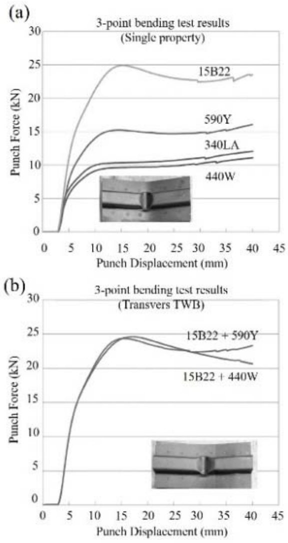

Fig. 11. Three-point bending test results of samples with a closed groove: (a) uniform blank; and (b) transversely welded TWBs

Table 4 lists the three-point bending test experimental results of a uniform blank and transverse and longitudinal welded TWBs with closed or open grooves.

Table 4. Three-point bending test results of the uniform blank with transverse and longitudinal TWBs with a closed or open groove

Blank	Max. Force (kN)		Energy Absorption (J)	
	opening groove	closing groove	opening groove	closing groove
15B22	18	25	516	783
340LA	10	10.5	326	369
440W	9.3	9.7	295	340
590Y	12.8	15.2	368	506
15B22+340LA Transverse TWB	14.4		388	
15B22+340LA Longitudinal TWB	11.9	17.6	354	584
15B22+440W Transverse TWB	13.8	24.6	374	769
15B22+440W Longitudinal TWB	11.7	17.1	340	566
15B22+590Y Transverse TWB	16.9	24.4	488	780
15B22+590Y Longitudinal TWB		19.4		634

It is clearly revealed in Fig.11(a) that the maximum punch force depends on the material strength of the specimen for uniform blanks, ranking from high to low by 15B22, 590Y, 340LA, and 440W. It is also observed that the punch force of TWB with an open groove, either transverse or longitudinal welded, is determined by the strength of the soft material. As for the energy absorption, it is also noted that the strength of hard and soft materials dominates the performance within the deformation range produced in the three-point bending test. However, a relatively large deformation is considered in the practical application for evaluating the energy absorption performance. Since 15B22 possesses a small elongation of typically 7%~8% after hot stamping, the comparison of energy absorption mainly focuses on the TWBs. The finite element simulation results of the three-point bending tests for all types of specimens are shown in Table 5. The simulation results of punch force and energy absorption display the same trend as those demonstrated by experimental results. The data obtained from the simulations also agree well with those from experiments.

Table 5. Three-point bending simulation results of the uniform blank with transverse and longitudinal TWBs with a closed or open groove

Blank	Max. Force (kN)		Energy Absorption (J)	
	opening groove	closing groove	opening groove	closing groove
15B22	18.9	26.7	575	852
340LA	10.4	11.5	308	363
440W	9.5	10.7	292	338
590Y	13.2	16.4	386	521
15B22+340LA Transverse TWB	13.9		350	
15B22+340LA Longitudinal TWB	12.8	19.5	367	549
15B22+440W Transverse TWB	13.4	25.9	336	802
15B22+440W Longitudinal TWB	12.5	18.3	321	537
15B22+590Y Transverse TWB	16.4	26.1	474	813
15B22+590Y Longitudinal TWB		20.5		593

To study the influence of weld line orientation on energy absorption, hot-stamped U-hat-shaped blanks (transverse or longitudinal weld line) were subjected to three-point tests, from which load-displacement curves were derived. As shown in Fig. 12, the energy absorption capacity of longitudinal TWBs was lower than that of their transverse TWB counterparts. When the longitudinal TWBs underwent deformation, the punch came into contact with both the soft and hard areas; however, punch pressure had a more pronounced effect on the soft zone material. Accordingly, the punch pressure of longitudinal TWB 15B22+590Y exceeded that of the TWB 15B22+440W. When the transverse TWBs underwent deformation, the punch came into contact only with the material in the hard area, such that the energy absorption capacity was determined entirely by the 15B22. Taken together, the transverse TWB exhibits a more favorable energy absorption performance than that of the longitudinal TWB.

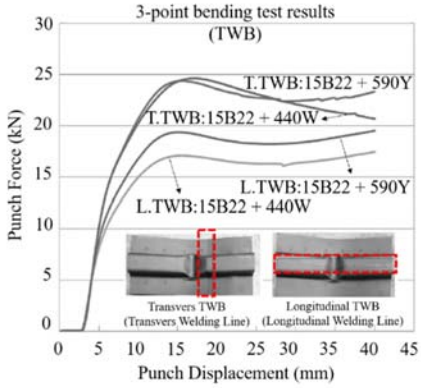

Fig. 12. Comparison of three-point bending test results of transverse and longitudinal TWBs with a closed groove

Experimental results of hot-stamped TWBs in the form of a half-section B-pillar

In this experiment, hot stamping was used to fabricate half-sectioned TWB B-pillars. The hard zone material (15B22) was respectively combined with soft zone materials of 340LA, 440W, and 590Y. The weld line of the TWBs did not crack under the effects of stamp forming, as shown in Fig. 13.

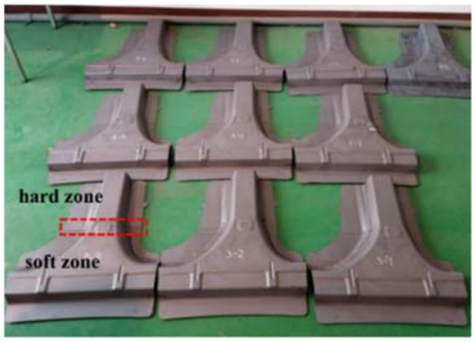

Fig. 13. TWB half-section B-pillar used in the hot-stamping experiment

After hot stamping, variations in the mechanical properties within the 15B22 area and the extent of deformation within the hard zone both decreased. The tensile strength of the resulting samples exceeded 1500 MPa, and elongation exceeded 8%. The tensile strength of 340LA and 440W was between 600 and 700 MPa, whereas the tensile strength of 590Y was 1000 MPa. Figure 14 illustrates the part of the specimens from which cuts were obtained. Table 6 list the test results of the topmost section of each test piece. The material compositions of the TWBs were shown to profoundly influence the mechanical properties of the component after hot stamping. Overall, it appears that soft zone material should be selected in accordance with the strength requirements of the component.

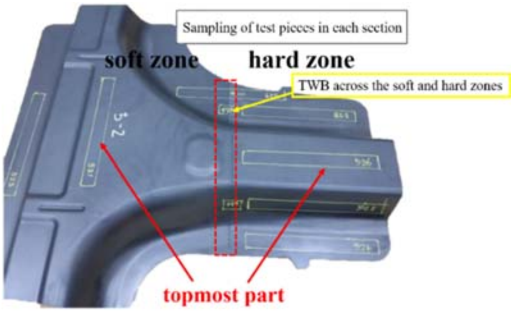

Fig. 14. Sections of half-section B-pillar examined in the hot-stamping experiment

Table 6. Test results of the topmost portion of hot-stamped TWB half-section B-pillar sample

		YS (MPa)	TS (MPa)	EL (%)
hard zone	15B22	1088	1540	8.3
soft zone	340LA	436	600	16.5
	440W	473	654	13.5
	590Y	834	1062	9.6

Hot stamping was shown to create various metallographic structures in the soft zones (340LA, 440W, and 590Y) of the TWB half-section B-pillars (see Fig. 15). Overall, the grains in the 440W were the largest, and the 340LA and 440W presented the lowest ferrite hardness and strength. The 590Y presented the high hardness indicative of the metallographic structures of pearlite and bainite. Figure 16 illustrates the hardness distribution across the soft and hard zones after hot stamping.

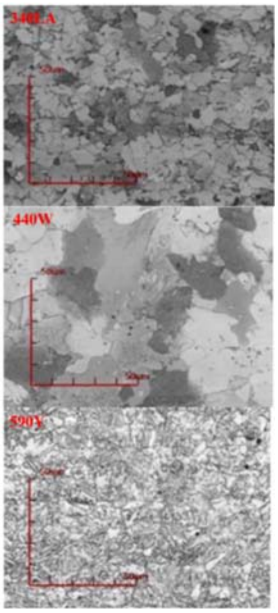

Fig. 15. Metallographic structure of soft area at the high point of the TWBs after hot stamping

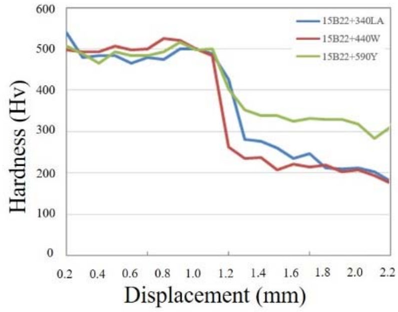

Fig. 16. Hardness distribution across soft and hard zones after hot stamping

Figures 17 to 19 illustrate the metallographic structure across the soft and hard regions of TWBs after hot stamping. The heat-affected zone of the weld bead was extremely narrow, and the external metallographic structure of fusion lines did not differ from that of the base metal, no other transitional metallographic structures formed outside the weld bead. The metallographic structure at the center of the weld bead was similar to that of the base metal in the soft zone; however, the grains were more refined. A narrow band of martensite/ bainite structures was observed near the fusion line of the 15B22 hard zone. Martensite was observed mainly in the weld bead of 15B22+590Y samples. The microstructure of the weld bead in 15B22+340LA and 15B22+440W samples comprised mainly ferrite. In the hot-stamped TWBs, the martensite/ bainite microstructure in the weld bead (due to rapid cooling after laser welding) changed to pearlite or ferrite (due to slow cooling after hot stamping). Thus, the material selected for the soft zone was the main factor influencing the properties of the weld bead after hot stamping.

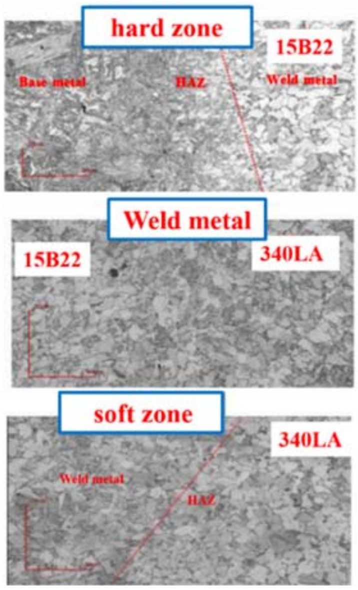

Fig. 17. Metallographic structure of 15B22+340LA across soft and hard regions after hot stamping

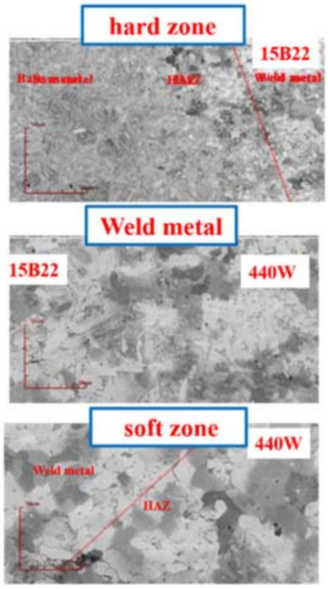

Fig. 18. Metallographic structure of 15B22+440W across the soft and hard regions after hot stamping

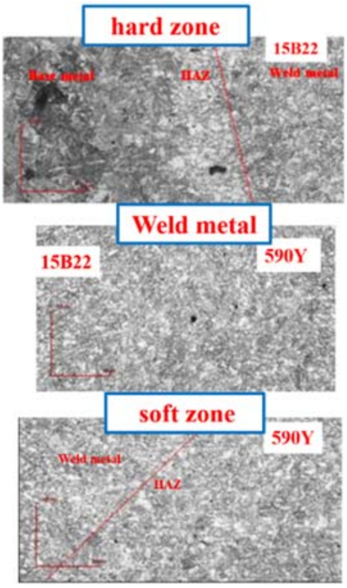

Fig. 19. Metallographic structure of 15B22+590Y across soft and hard regions after hot stamping

CONCLUSIONS

This study conducted a series of hot-stamping experiments on TWBs. When hot stamping was applied to a uniform specimen (one homogenous material), energy absorption capacity was directly proportional to the strength of the material, as revealed in three-point bending tests. Subjecting TWB U-hat-shaped specimens to pressure led to deformation only in the soft area (i.e., the hard area was preserved). This underlines the importance of selecting materials for strong and weak TWB regions when seeking to maximize the crashworthiness of a B-pillar. In experiments involving half-section B-pillars, the metallographic structure of the soft zone differed considerably from that of the 15B22 hard zone after hot stamping. Hot stamping was shown to transform 15B22 into martensite, with a corresponding increase in strength. Hot stamping transformed 340LA and 440W into ferrite, thereby decreasing the strength of the material in the weak area. Hot stamping transformed 590Y into pearlite and bainite, resulting in strength values far exceeding those of 340LA and 440W.

ACKNOWLEDGMENTS

The authors wish to thank the Ministry of Science and Technology of Taiwan, ROC, for the grant under project #MOST106-2622-8-006-001. The authors would also like to thank the Metal Industries Research & Development Centre for supporting the experiment apparatus and ESI for the PAM-STAMP simulation software.

REFERENCES

Xing, Z. W., Bao, J., and Yang, Y. Y., “Numerical simulation of hot stamping of quenchable boron steel,” *Mater. Sci. Eng. A*, Vol.499, pp.28-31 (2009).

Karbasian, H. and Tekkaya, A.E., “A review on hot stamping,” *J. Mater. Process. Technol.*, Vol.210, pp. 2103-2118 (2010).

Bariani, P. F., Bruschi, S., Ghiotti, A., and Turetta, A., “Testing formability in the hot stamping of HSS,” *CIRP Ann. Manuf. Technol.*, Vol.57, pp.265-268 (2008).

Eller, T. K., Greve, L., Andres, M. T., Medricky, M., Hatscher, A., Meinders, V. T., and van den Boogaard, A. H, “Plasticity and fracture modeling of quench-hardenable boron steel with tailored properties,” *J. Mater. Process. Technol.*, Vol.214, pp.1211-1227 (2014).

Li, M. F., Chiang, T. S., Tseng, J. H., and Tsai, C. N., “Hot stamping of door impact beam,” *Procedia Eng.*, Vol.81, pp. 1786-1791 (2014).

Taylor, T. and Clough, A., “Critical review of automotive hot-stamped sheet steel from an industrial perspective,” *Mater. Sci. Technol.*, Vol.34, No.7, pp. 809-861 (2018).

Wang, Z. J., Liu, P. X., Xu, Y., Wang, Y. L., and Zhang, Y. S., “Hot stamping of high strength steel with tailored properties by two methods,” *Procedia Eng.*, Vol.81, pp.1725-1730 (2014).

Hein, P. and Wilsius, J., “Status and Innovation Trends in Hot Stamping of USIBOR 1500 P,” *Steel Research Int.*, Vol.79, No.2, pp.85-91 (2008).

Mori, K. I., Kaido, T., Suzuki Y., Nakagawa, Y., and Abe, Y., “Combined process of hot stamping and mechanical joining for producing ultra-high strength steel patchwork components," *J. Manuf. Processes*, Vol.59, pp.444-455 (2020).

Merklein, M., Johannes, M., Lechner, M., and Kuppert, A., "A review on tailored blanks—Production, applications and evaluation," *J. Mater. Process. Technol.*, Vol.214, pp.151-164 (2014).

Tang, B. T., Yuan, Z. J., Cheng, G., Huang, L. L., Zheng, W., and Xie, H., "Experimental verification of tailor welded joining partners for hot stamping and analytical modeling of TWBs rheological constitutive in austenitic state," *Mater. Sci. Eng. A*, Vol.585, pp. 304-318 (2013).

Bok, H. H., Choi, J. W., Suh, D. W., Lee, M. G., and Barlat, F., "Stress development and shape change during press-hardening process using phase-transformation-based finite element analysis," *Int. J. Plast.*, Vol.73, pp. 142-170 (2015).

Múnera, D. D., Pic, A., Abou-Khalil, D., and Shmit, F., and Pinard, F., "Innovative Press Hardened Steel Based Laser Welded Blanks Solutions for Weight Savings and Crash Safety Improvements," *SAE Int. J. Mater. Manuf.*, Vol. 1, No. 1, pp. 472-479 (2009).

Choi, J. W., Lee, M. G., Barlat, F., Son, H. S., and Nam, J. B., "Hot Press Forming of Tailor Welded Blank: Experiments and FE Modeling," *ISIJ Int.*, Vol. 52, No. 11, pp. 2059-2068 (2012).

Kolleck, R., Vollmer, R., Both, C., and Breuer, A., "Investigation of Weld Seam Structures of Tailor Welded Blanks for Hot Stamping," *Key Eng. Mater.*, Vol.639, pp. 235-242 (2015).

Choi, H. S., Ko, D. C., and Kim, B. M., "Effect of Weld Line Orientation on Formability of Tailor Welded Blank of 22MnB5 at Elevated Temperature," *Adv. Mech. Eng.*, (2016).

Peister, C., George, R., Omer, K., Worswick, M. J., Malcolm, S., Dykeman, J., Yau, C., Soldaat, R., and Bernert, W., "Forming of an axially tailored automotive channel section through hot stamping of tailor-welded blanks," *J. Phys. Conf. Ser.*, Vol.896, (2017).

Song, Y. L., Han, Y., Hua, L., Lu, J., and Yu, C., "Optimal Design and Hot Stamping of B-Pillar Reinforcement Panel with Variable Strength based on Side Impact," *ICHSU*, pp. 320-326 (2015).

George, R., Bardelcik, A., and Worswick, M. J. "Hot forming of boron steels using heated and cooled tooling for tailored properties," *J. Mater. Process. Technol.*, Vol.212, pp. 2386-2399 (2012).

Pack, K. and Marcadet, S. J., "Numerical failure analysis of three-point bending on martensitic hat assembly using advanced plasticity and fracture models for complex loading," *Int. J. Solids Struct.*, pp. 144-159 (2016).

Peister, C., O'Keeffe, C., Imbert, J., Butcher, C., Worswick, M., Malcolm, S., Dykeman, J., Yau, C., Soldaat, R., and Bernert, W., "Dynamic and Quasi-Static Testing and Modeling of Hot Stamped Tailor-Welded Axial Crush Rails," *Proc.*, (2018).

Tang, B. T., Wu, F. X., Guo, N., Liu, J. Y., Ge, H. L., Bruschi, S., and Li, X. S., "Numerical modeling of ductile fracture of hot stamped 22MnB5 boron steel parts in three-point bending," *Int. J. Mech. Sci.*, Vol.188, (2020).

Merklein, M., Wieland, M., Lechner, M., Bruschi, S., and Ghiotti, A., "Hot stamping of boron steel sheets with tailored properties: A review," *J. Mater. Process. Technol.,* Vol.228, pp. 11-24 (2016).

ChiuHuang, C. K., Chiang M. F., and Lee P. K., "Numerical and Experimental Investigation on Hot Stamping of TWB B-Pillar," *Mater. Sci. Eng.*, Vol.967, (2020).

Arcelor Mittal, "Hot Stamping Steel solutions to answer CO_2 & Crash regulations evolution," (2016).

Chen, L. W., Chen, Y. H., and Hsu, Y. C., "A Tailored Tempering Process for CSC-15B22 Steel Sheet," *J. Manuf. Sci. Eng.*, Vol.140, (2018).

Mu, Y. H., Zhou, J., Wang, B. Y., Wang, Q. L., Ghiotti, A., and Bruschi, S., "Numerical simulation of hot stamping by partition heating based on advanced constitutive modelling of 22MnB5 behaviour," *Finite Elem. Anal. Des.*, pp.1–11 (2018).

Wang, Z. J., and Zhang, Y. S., "Investigation into the Hardness Prediction and Crashworthiness of the Local Tempered Parts," *ICHSU*, pp. 310-314 (2015).

Shi, D., Watanabe, K., Naito, J., Funada, K., and Yasui, K., "Design optimization and application of hot-stamped B pillar with local patchwork blanks," *Thin-Walled Structures*, Vol.170, pp. 108523 (2022).

熱沖壓裁縫式焊接鋼板之探討

李建興
國立陽明交通大學機械工程學系

洪景華
國立陽明交通大學機械工程學系

李炳坤 邱黃正凱
中鋼公司鋼鐵研究發展處產品應用技術組

陳復國
國立臺灣大學機械工程學系

摘 要

汽車行業不斷尋求在不影響安全性的情況下減輕車輛重量。汽車中使用的 B 柱在其底部區域需要更高的能量吸收能力，同時在上部區域保留麻田散鐵結構以防止變形。這導致了拼焊板(TWBs)的發展，其中單一汽車結構件具有多種機械性能。本研究進行了一系列的裁縫式焊接鋼板熱沖壓實驗之探討，包括帽型試片和半截 B 柱。在三點彎曲試驗表明，TWBs 熱沖壓試件的能量吸收能力與材料的強度成正比。裁縫式焊接板材強弱材料適度搭配可引導結構件的變形行為，以符合車體受撞功能需求。